DOI: 10.3901/CJME.2013.01.035, available online at www.springerlink.com; www.cjmenet.com; www.cjmenet.com.cn

Design and Analysis of a New AUV's Sliding Control System Based on Dynamic Boundary Layer

GAO Fudong[1, 2, *], PAN Cunyun[1], and HAN Yanyan[3]

1 *College of Mechatronic Engineering and Automation, National University of Defense Technology, Changsha 410073, China*
2 *Department of Shipboard Aviation Security and Station Management, Naval Aeronautical and Astronautical University, Qingdao 266041, China*
3 *SANY Heavy Industry Co. Ltd, Changsha 410100, China*

Received January 18, 2012; revised June 12, 2012; accepted June 19, 2012

Abstract: The new AUV driven by multi-vectored thrusters not only has unique kinematic characteristics during the actual cruise but also exists uncertain factors such as hydrodynamic coefficients perturbation and unknown interference of tail fluid, which bring difficult to the stability of the AUV's control system. In order to solve the nonlinear term and unmodeled dynamics existing in the new AUV's attitude control and the disturbances caused by the external marine environment, a second-order sliding mode controller with double-loop structure that considering the dynamic characteristics of the rudder actuators is designed, which improves the robustness of the system and avoids the control failure caused by the problem that the design theory of the sliding mode controller does not match with the actual application conditions. In order to avoid the loss of the sliding mode caused by the amplitude and rate constraints of the rudder actuator in the new AUV's attitude control, the dynamic boundary layer method is used to adjust the sliding boundary layer thickness so as to obtain the best anti-chattering effects. Then the impacts of system parameters, rudder actuator's constraints and boundary layer on the sliding mode controller are computed and analyzed to verify the effectiveness and robustness of the sliding mode controller based on dynamic boundary layer. The computational results show that the original divergent second-order sliding mode controller can still effectively implement the AUV's attitude control through dynamically adjusting the sliding boundary layer thickness. The dynamic boundary layer method ensures the stability of the system and does not exceed the amplitude constraint of the rudder actuator, which provides a theoretical guidance and technical support for the control system design of the new AUV in real complex sea conditions.

Key words: dynamic boundary layer, new AUV, nonlinear system, sliding mode control

1 Introduction

AUVs are promising vehicles for navy use because they can fulfill many missions such as assaults, communications and obviating torpedoes. In order to meet the needs of future high-tech naval warfare, fastness and seakeeping of the AUVs become the basic premise of safe navigation and effective use of weapons. The multi-moving state AUV in this paper makes use of the flexible transmission shaft based on spherical gear as the kinetic source equipment[1], on the end of that a new wheel propeller is installed. The whole equipment can achieve four functions such as wheels, legs, thrusters and course control based on the characteristics of spatial deflexion and continual circumgyratetion of the flexible transmission shaft. The rudders and vectored thrusters are used to control the course at high speed and low speed respectively. The typical motions of the AUV are shown in Fig. 1[2].

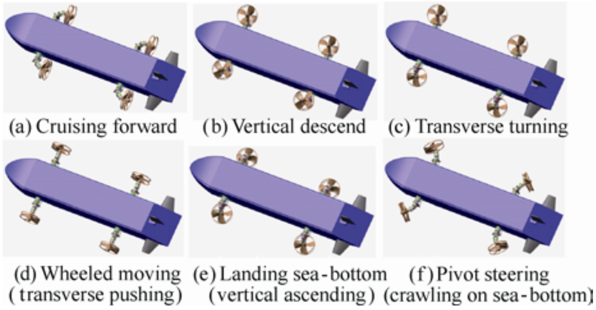

Fig. 1. Typical motions of the vectored thruster AUV

As AUVs are subject to the larger interference effect from underwater environment, in order to ensure the stability of the new AUV, it needs a good control system

* Corresponding author. E-mail: gaofudong2005@163.com

This project is supported by National Hi-tech Research and Development Program of China (863 Program, Grant No. 2006AA09Z235), and Hunan Provincial Innovation Foundation for Postgraduate of China (Grant No. CX2009B003)

with strong robustness and anti-jamming capability. However, the new AUV is a highly non-linear, time-varying and strong coupling system. It is difficult to establish an accurate motion model considering the uncertainty of environmental interference. Therefore, the control method used in the new AUV should get rid of the dependence on the precise mathematical model. Among many control methods, sliding mode control has strong robustness about parameters change, uncertainties and external disturbances, so sliding mode control is very effective to solve the control problem of the AUVs in complex sea conditions[3].

In real systems, the high frequency chattering will occur along with the sliding mode in sliding mode control system due to time lag switch, spatial lag switch, system inertia, system delay, measurement error and other factors. The chattering not only affects the control accuracy and increases energy consumption but also can arouse the high-frequency unmodeled dynamics of the system easily, which undermines the system's performance, causes the system's oscillation and instability and damages the controller unit[4]. In the specific applications of the AUV, infinite frequency switching control can not be carried out to maintain the ideal sliding mode of the system due to the physical constraints of the rudder actuator, which leads to the loss of the sliding mode[5]. In many references[6–9], the dynamic characteristics of the rudder actuator are usually not considered in the sliding mode controller design of the AUV's attitude, which may cause the failure of practical application due to that the rudder actuator can not achieve the theory requirements of the sliding mode controller. At present, domestic and foreign scholars introduce concepts including "quasi-sliding mode" and "boundary layer" in the sliding mode controller design to achieve a quasi-sliding mode control, which uses saturation function instead of the switching function to prevent and reduce the chattering of the system effectively through using normal sliding mode control beyond the boundary layer and using continuous state feedback control in the boundary layer. CHEN, et al[10], proposed an on-line adjustment algorithm of the boundary layer thickness based on the system state norm with considering reducing control signal's chattering and ensuring tracking accuracy aim at uncertain linear systems. VICENTE, et al[11], proposed a new dynamic sliding mode control through designing a new non-linear switching function s with saturation function so as to eliminate the chattering of sliding mode in reaching stage, which realizes global robust sliding mode control and solves a class of chattering control problem of nonlinear mechanical systems effectively. SESHAGIRI, et al[12], used integral control in the boundary layer to reduce the boundary layer thickness, which obtains the steady-state error and avoids the chattering. In this paper, a second order sliding mode controller with double-loop structure based on dynamic boundary layer is proposed to control the AUV's attitude with considering the dynamic characteristics and the magnitude and rate limits of the rudder actuator, which synthesizes the advantages of reducing system's chattering of the above method. The effectiveness and robustness of the sliding mode controller are verified through analyzing the impacts of system parameters, rudder actuator constraints and boundary layer on the sliding mode controller.

2 Sliding Mode Control Algorithm for the Nonlinear System

The motion process of the new AUV in the complex sea conditions is a complicated nonlinear dynamic system. In order to describe the movement of the new AUV, the inertial coordinate system E-$\xi\eta\zeta$ and body-fixed coordinate system B-xyz are used, as shown in Fig. 2[13]. Considering the dynamic characteristics of the rudder actuator, the dynamic equations with unmodeled uncertainties of the new AUV are established, which can be expressed as

$$\dot{\boldsymbol{\eta}}_2 = \boldsymbol{f}_1(\boldsymbol{\eta}_2, \boldsymbol{\delta}) + \Delta\boldsymbol{f}_1(\boldsymbol{\eta}_2, \boldsymbol{\delta}) + (\boldsymbol{b}_1(\boldsymbol{\eta}_2) + \Delta\boldsymbol{b}_1(\boldsymbol{\eta}_2))\boldsymbol{v}_2, \quad (1)$$

$$\dot{\boldsymbol{v}}_2 = \boldsymbol{f}_2(\boldsymbol{\eta}_2, \boldsymbol{v}_2) + \Delta\boldsymbol{f}_2(\boldsymbol{\eta}_2, \boldsymbol{v}_2) + (\boldsymbol{b}_2(\boldsymbol{\eta}_2) + \Delta\boldsymbol{b}_2(\boldsymbol{\eta}_2))\boldsymbol{\delta}, \quad (2)$$

$$\dot{\boldsymbol{\delta}} = -\boldsymbol{K}_\delta(\boldsymbol{\delta} - \boldsymbol{u}), \quad (3)$$

where $\boldsymbol{\eta}_2=(\phi\ \ \theta\ \ \psi)^{\mathrm{T}}$ is the attitude vector in the inertial coordinate system, $\boldsymbol{v}_2=(p\ \ q\ \ r)^{\mathrm{T}}$ is the angular velocity vector in the body-fixed coordinate system, $\boldsymbol{\delta}=(\delta_{\mathrm{p}}\ \ \delta_{\mathrm{r}})^{\mathrm{T}}$ describes the horizontal rudder angle and vertical rudder angle, $\boldsymbol{u}\in\mathbf{R}^2$ is the control input of the rudder actuator, $\boldsymbol{f}_1(\boldsymbol{\eta}_2,\ \boldsymbol{\delta})\in\mathbf{R}^3$, $\boldsymbol{f}_2(\boldsymbol{\eta}_2,\ \boldsymbol{v}_2)\in\mathbf{R}^3$ are differentiable functions, $\boldsymbol{b}_1(\boldsymbol{\eta}_2)\in\mathbf{R}^{3\times3}$, $\boldsymbol{b}_2(\boldsymbol{\eta}_2)\in\mathbf{R}^{3\times2}$ and $\boldsymbol{K}_\delta$ are known matrixes, $\Delta\boldsymbol{f}_1(\boldsymbol{\eta}_2,\ \boldsymbol{\delta})\in\mathbf{R}^3$, $\Delta\boldsymbol{f}_2(\boldsymbol{\eta}_2,\ \boldsymbol{v}_2)\in\mathbf{R}^3$, $\Delta\boldsymbol{b}_1(\boldsymbol{\eta}_2)\in\mathbf{R}^{3\times3}$, $\Delta\boldsymbol{b}_2(\boldsymbol{\eta}_2)\in\mathbf{R}^{3\times2}$ are bounded smooth perturbation term caused by model uncertainties. The amplitude and rate constraints of rudder actuator can be expressed as

$$\left|\delta_i\right| \leqslant \delta_{\mathrm{m}}, \quad \left|\dot{\delta}_i\right| \leqslant \bar{\delta}_{\mathrm{m}}. \quad (4)$$

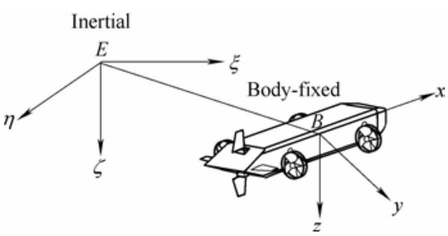

Fig. 2. Inertial and body-fixed coordinate systems

Given a real-time attitude angle reference trajectory, a second-order sliding mode controller with double-loop structure based on attitude angle and angular velocity is designed. Firstly, the angular velocity reference command is computed out through the attitude angular deviation based on the outer-loop sliding mode controller. Then the input command of rudder angle $\boldsymbol{u}_c$ is computed out through the angular velocity reference command based on the inner-loop sliding mode controller. In order to ensure the system state expressed by motion equations tracking the attitude angle reference command progressively, According to the principle of trajectory tracking control, we define

$$\lim_{t\to\infty}\left|\eta_{2ri}(t)-\eta_{2i}(t)\right|=0,\ i=1,2,3. \tag{5}$$

2.1 Outer-loop sliding mode control algorithm design for attitude angle

According to the attitude dynamic Eq. (1), the outer-loop sliding mode controller is designed with attitude angular deviation to compute the angular velocity control command $\boldsymbol{v}_{2c}$. The tracking error of attitude angle is defined as

$$e_i=\eta_{2ri}(t)-\eta_{2i}(t). \tag{6}$$

The sliding surface is designed as

$$\boldsymbol{s}=\boldsymbol{e}+c\int_0^t \boldsymbol{e}\mathrm{d}t, \tag{7}$$

where $\boldsymbol{s}\in\mathbf{R}^3$, $\boldsymbol{e}=(e_1\ e_2\ e_3)^{\mathrm{T}}$. So we can get

$$\begin{aligned}\dot{\boldsymbol{s}}=\dot{\boldsymbol{\eta}}_2\ (t_r)-\boldsymbol{f}_1(\boldsymbol{\eta}_2,\boldsymbol{\delta})-\Delta\boldsymbol{f}_1(\boldsymbol{\eta}_2,\boldsymbol{\delta})-\\(\boldsymbol{b}_1(\boldsymbol{\eta}_2)+\Delta\boldsymbol{b}_1(\boldsymbol{\eta}_2))\boldsymbol{v}_2+c\boldsymbol{e}.\end{aligned} \tag{8}$$

Defining $\dot{\boldsymbol{s}}=\boldsymbol{0}$ and assuming the uncertain terms are zero, the equivalent control law can be expressed as

$$\boldsymbol{v}_{2\mathrm{eq}}=\boldsymbol{b}_1(\boldsymbol{\eta}_2)^{-1}\left[\dot{\boldsymbol{\eta}}_2\ (t_r)-\boldsymbol{f}_1(\boldsymbol{\eta}_2,\boldsymbol{\delta})+c\boldsymbol{e}\right]. \tag{9}$$

The switching control law is designed as

$$\boldsymbol{v}_{2\mathrm{n}}=\mu\boldsymbol{b}_1(\boldsymbol{\eta}_2)^{-1}\mathrm{sgn}(\boldsymbol{s}),\ \mu>0, \tag{10}$$

where $\mathrm{sgn}(\boldsymbol{s})=(\mathrm{sgn}(s_1)\quad \mathrm{sgn}(s_2)\quad \mathrm{sgn}(s_3))^{\mathrm{T}}$.
Hence, the total control law can be written as

$$\begin{aligned}\boldsymbol{v}_{2\mathrm{c}}=\boldsymbol{v}_{2\mathrm{eq}}+\boldsymbol{v}_{2\mathrm{n}}=\boldsymbol{b}_1(\boldsymbol{\eta}_2)^{-1}[\dot{\boldsymbol{\eta}}_{2\mathrm{r}}(t)-\boldsymbol{f}_1(\boldsymbol{\eta}_2,\boldsymbol{\delta})+c\boldsymbol{e}]+\\\mu\boldsymbol{b}_1(\boldsymbol{\eta}_2)^{-1}\mathrm{sgn}(\boldsymbol{s}).\end{aligned} \tag{11}$$

In order to analyze the system's stability, the Lyapunov function is defined as[14]

$$V=\frac{1}{2}\boldsymbol{s}^{\mathrm{T}}\boldsymbol{s}. \tag{12}$$

From Eq. (11) and Eq. (8), the derivative of Lyapunov function can be written as

$$\dot{V}=\boldsymbol{s}^{\mathrm{T}}\dot{\boldsymbol{s}}=\boldsymbol{s}^{\mathrm{T}}\left\{\boldsymbol{A}(\boldsymbol{\eta}_2,\boldsymbol{\delta})-\mu\left[\boldsymbol{I}+\boldsymbol{B}(\boldsymbol{\eta}_2)\right]\mathbf{sgn}(\boldsymbol{s})\right\}, \tag{13}$$

where $\boldsymbol{A}(\boldsymbol{\eta}_2,\boldsymbol{\delta})=-\Delta\boldsymbol{f}_1(\boldsymbol{\eta}_2,\boldsymbol{\delta})-\boldsymbol{B}(\boldsymbol{\eta}_2)[\dot{\boldsymbol{\eta}}_{2\mathrm{r}}+c\boldsymbol{e}-\boldsymbol{f}_1(\boldsymbol{\eta}_2,\boldsymbol{\delta})]$,

$$\boldsymbol{B}(\boldsymbol{\eta}_2)=\Delta\boldsymbol{b}_1(\boldsymbol{\eta}_2)\boldsymbol{b}_1(\boldsymbol{\eta}_2)^{-1}.$$

Defining the boundary conditions of $\boldsymbol{A}(\boldsymbol{\eta}_2,\boldsymbol{\delta})$ and $\boldsymbol{B}(\boldsymbol{\eta}_2)$ are $|A_i|\leqslant a_i$, $|B_{ij}|\leqslant b_{ij}$, $\sum_{j=1}^{3}b_{ij}<1$, respectively, we can get

$$\dot{V}\leqslant\sum_{i=1}^{3}|s_i|\cdot\left[a_i-\mu\left(1-\sum_{j=1}^{3}b_{ij}\right)\right]. \tag{14}$$

Hence, the existence condition of the sliding mode holds because the Lyapunov function derivative is negative when μ meets the following condition:

$$\mu>\max_{i=1,2,3}\left[a_i\Big/\left(1-\sum_{j=1}^{3}b_{ij}\right)\right]. \tag{15}$$

With the condition of sufficient control, Eq. (11) and Eq. (15) can ensure the asymptotic stability of the sliding surface $\boldsymbol{s}$ in dynamic Eq. (7) and make the moving point out the sliding surface reach the sliding surface in limited time. As the angular velocity control command given by the sliding mode controller for attitude angle in Eq. (11) is not continuous, so the sliding mode controller for angular velocity can not complete the tracking control. In order to solve this problem, a saturation function $\mathrm{sat}(\boldsymbol{s}/\boldsymbol{\gamma})$ is used to linearize the noncontinuous switch item $\mathrm{sgn}(\boldsymbol{s})$ in the sliding mode controller for attitude angle[15], which can be expressed as

$$\mathrm{sat}\left(\frac{\boldsymbol{s}}{\boldsymbol{\gamma}}\right)=\left[\mathrm{sat}\left(\frac{s_1}{\gamma_1}\right)\quad\mathrm{sat}\left(\frac{s_2}{\gamma_2}\right)\quad\mathrm{sat}\left(\frac{s_3}{\gamma_3}\right)\right]^{\mathrm{T}}, \tag{16}$$

$$\mathrm{sat}\left(\frac{s_i}{\gamma_i}\right)=\begin{cases}1, & s_i>\gamma_i,\\ \dfrac{s_i}{\gamma_i}, & |s_i|\leqslant\gamma_i,\\ -1, & s_i<-\gamma_i.\end{cases} \tag{17}$$

where γ_i is the boundary layer thickness of the sliding surface. It can be seen from the saturation function, linear feedback control is used in the boundary layer of the system and switching control is used out the boundary layer, which reduces or avoids the chattering of the sliding mode.

2.2 Inner-loop sliding mode control algorithm design for angular velocity

From Eq. (2) and Eq. (3), the control input $\boldsymbol{u}$ is adjusted to track the angular velocity control command $\boldsymbol{v}_{2c}$ generated by outer-loop sliding mode controller for attitude angular, which can be expressed as

$$\lim_{t\to\infty}\left|v_{2ci}-v_{2i}\right|=0,\ i=1,2,3. \tag{18}$$

The tracking error of angular velocity command is defined as

$$e_i' = v_{2ci} - v_{2i} \,. \tag{19}$$

Then the PID-structure sliding surface of the system is designed as

$$\boldsymbol{\sigma} = \dot{\boldsymbol{e}}' + c_1\boldsymbol{e}' + c_2\int_0^t \boldsymbol{e}'\mathrm{d}t \,, \tag{20}$$

where $\boldsymbol{\sigma}\in\mathbf{R}^3$, $\boldsymbol{e}' = (e_1' \quad e_2' \quad e_3')^{\mathrm{T}}$. So the kinematic equation of the system in $\boldsymbol{\sigma}$ subspace can be written as

$$\dot{\sigma} = \boldsymbol{\Gamma}(\boldsymbol{\eta}_2, \boldsymbol{v}_2, \boldsymbol{\delta}) - (\boldsymbol{b}_2 + \Delta\boldsymbol{b}_2)\dot{\boldsymbol{\delta}} \,, \tag{21}$$

where

$$\boldsymbol{\Gamma}(\boldsymbol{\eta}_2, \boldsymbol{v}_2, \boldsymbol{\delta}) = \ddot{\boldsymbol{v}}_{2\mathrm{c}} + c_1\dot{\boldsymbol{v}}_{2\mathrm{c}} + c_2\boldsymbol{e}' - \frac{\mathrm{d}}{\mathrm{d}t}(\boldsymbol{f}_2 + \Delta\boldsymbol{f}_2) - c_1(\boldsymbol{f}_2 + \Delta\boldsymbol{f}_2) - \left[\frac{\mathrm{d}}{\mathrm{d}t}(\boldsymbol{b}_2 + \Delta\boldsymbol{b}_2) + c_1(\boldsymbol{b}_2 + \Delta\boldsymbol{b}_2)\right]\boldsymbol{\delta} \,.$$

Defining $\dot{\sigma} = 0$ and assuming the uncertain items are all zero, the equivalent control law can be written as Defining $\dot{\sigma} = 0$ and assuming the uncertain items are all zero, the equivalent control law can be written as

$$\dot{\boldsymbol{\delta}}_{\mathrm{eq}} = \boldsymbol{b}_2^{-1}\left[\ddot{\boldsymbol{v}}_{2\mathrm{c}} + c_1\dot{\boldsymbol{v}}_{2\mathrm{c}} + c_2\boldsymbol{e}' - \frac{\mathrm{d}\boldsymbol{f}_2}{\mathrm{d}t} - c_1\boldsymbol{f}_2 - \left(\frac{\mathrm{d}\boldsymbol{b}_2}{\mathrm{d}t} + c_1\boldsymbol{b}_2\right)\boldsymbol{\delta}\right] = \boldsymbol{b}_2^{-1}\hat{\boldsymbol{\Gamma}}(\boldsymbol{\eta}_2, \boldsymbol{v}_2, \boldsymbol{\delta}) \,. \tag{22}$$

In order to ensure the existence condition of the sliding mode holding, the sliding mode control law for angular velocity with additional switching function can be designed as

$$\dot{\boldsymbol{\delta}} = \dot{\boldsymbol{\delta}}_{\mathrm{eq}} + \boldsymbol{k}\cdot\mathrm{sgn}(\boldsymbol{\sigma}), \tag{23}$$

where $\boldsymbol{k} = \begin{pmatrix} k_1 & 0 & 0 \\ 0 & k_2 & 0 \end{pmatrix}$, $k_i > 0,\ i = 1, 2,$

sgn($\boldsymbol{\sigma}$)=(sgn(σ_1) sgn(σ_2) sgn(σ_3))$^{\mathrm{T}}$.

In order to verify the system's asymptotic stability, the Lyapunov function is designed as

$$V = \frac{1}{2}\boldsymbol{\sigma}^{\mathrm{T}}\boldsymbol{\sigma} \,. \tag{24}$$

So the derivative of the Lyapunov function can be expressed as

$$\dot{V} = \boldsymbol{\sigma}^{\mathrm{T}}\dot{\boldsymbol{\sigma}} = \boldsymbol{\sigma}^{\mathrm{T}}\left[\boldsymbol{\Gamma}(\boldsymbol{\eta}_2, \boldsymbol{v}_2, \boldsymbol{\delta}) - (\boldsymbol{b}_2 + \Delta\boldsymbol{b}_2)\dot{\boldsymbol{\delta}}\right]. \tag{25}$$

Defining $\boldsymbol{G}(\boldsymbol{\eta}_2) = \boldsymbol{\tau} - \Delta\boldsymbol{b}_2\boldsymbol{b}_2^{-1}\hat{\boldsymbol{\Gamma}}$, $\boldsymbol{H}(\boldsymbol{\eta}_2) = \boldsymbol{b}_2 + \Delta\boldsymbol{b}_2$, $\boldsymbol{\tau} = \boldsymbol{\Gamma} - \hat{\boldsymbol{\Gamma}}$, substituting Eq. (23) into Eq. (25), we can get

$$\dot{V} = \boldsymbol{\sigma}^{\mathrm{T}}\left[\boldsymbol{G} - \boldsymbol{H}\cdot\boldsymbol{k}\cdot\mathbf{sgn}(\sigma)\right]. \tag{26}$$

Assuming the maximum of the functions $\boldsymbol{G}(\boldsymbol{\eta}_2)$ and $\boldsymbol{H}(\boldsymbol{\eta}_2)$ including unmodeled uncertain items are $|G_i| \leqslant g_i$ and $|H_{ij}| \leqslant h_{ij}$, respectively, the inequality can be obtained:

$$\dot{V} \leqslant \sum_{i=1}^{2}|\boldsymbol{\sigma}_i|(g_i - k_i h_{ij}). \tag{27}$$

Therefore, the gain condition insuring the derivative of the Lyapunov function negative can be expressed as

$$k_i > \frac{g_i}{h_{ij}} \,. \tag{28}$$

Eq. (23) and Eq. (28) can ensure the existence of the sliding mode on the sliding surface $\boldsymbol{\sigma}$. Furthermore, the state beyond the sliding surface will reach the sliding surface in limited time. From Eq. (3) and Eq. (23), the input control law of the rudder angle can be expressed as

$$u_i = \delta_i + \frac{1}{k_\delta}\left[\dot{\delta}_{\mathrm{eq}i} + k_i\mathrm{sgn}(\sigma_i)\right], i = 1, 2. \tag{29}$$

The same as the outer-loop sliding mode controller, the saturation function is used to substitute the discontinuous switching function sgn(σ_i) in Eq. (29) so as to avoid the phenomenon of control chattering. If the boundary layer thickness of the sliding surface is defined as π_i, we can get

$$\mathrm{sat}\left(\frac{\sigma_i}{\pi_i}\right) = \begin{cases} 1, & \sigma_i > \pi_i, \\ \dfrac{\sigma_i}{\pi_i}, & |\sigma_i| \leqslant \pi_i, \quad i = 1, 2. \\ -1, & \sigma_i < -\pi_i. \end{cases} \tag{30}$$

Finally, the continuous sliding mode control law of the rudder angle input can be expressed as

$$u_i = \delta_i + \frac{1}{k_\delta}\left[\dot{\delta}_{\mathrm{eq}i} + k_i\mathrm{sat}\left(\frac{\sigma_i}{\pi_i}\right)\right], \quad i = 1, 2. \tag{31}$$

When $\dot{\boldsymbol{\delta}}_{\mathrm{eq}} = 0$, we can get

$$u_i = \delta_i + \frac{1}{k_\delta}k_i\mathrm{sat}\left(\frac{\sigma_i}{\pi_i}\right), \quad i = 1, 2. \tag{32}$$

The continuous sliding mode control law of the rudder angle can not ensure that the states converge to the sliding surface. However, the attracting domain of the sliding surface can be determined through analyzing the derivative of Lyapunov function[16–17]. The derivative of Lyapunov function can be written as

$$\dot{V}=\boldsymbol{\sigma}^{\mathrm{T}}\left[\boldsymbol{G}-\boldsymbol{H}\cdot\boldsymbol{\rho}\cdot\mathrm{sat}\left(\frac{\boldsymbol{\sigma}}{\boldsymbol{\pi}}\right)\right], \tag{33}$$

where $\boldsymbol{\rho}$=diag$\{\rho_i\}$, $\rho_i>0$. In order to ensure $\dot{V}<0$, the range of the gain ρ_i is selected as

$$\rho_i=\begin{cases} k_i, & |\sigma_i|\leqslant\pi_i, \\ \dfrac{k_i\sigma_i}{\pi_i}, & |\sigma_i|>\pi_i, \end{cases} \quad i=1,2. \tag{34}$$

It can be seen from Eq. (34) that the moving points beyond the sliding surface can reach sliding surface $|\sigma_i|=\pi_i$ in a limited time and arrive the smaller area $|\sigma_i|\leqslant \rho_i\pi_i/k_i$. The solution of Eq. (21) is uniformly bounded. Therefore, the continuous sliding mode control law of rudder angle ensures the robustness of the sliding surface $\boldsymbol{\sigma}$ because the motion form of the states in attracting area $|\sigma_i|\leqslant\pi_i$ conforms to the following inequality, which is written as

$$\left|\dot{e}_i'+c_1e_i'+c_2\int_0^t e_i'\mathrm{d}t\right|\leqslant\pi_i, \quad i=1,2,3. \tag{35}$$

If Eq. (4) is considered, the continuous sliding mode control law of the rudder angle in Eq. (31) can be expressed as

$$u_i=\begin{cases} \delta_{\mathrm{m}}, & \lambda_{1i}>\delta_{\mathrm{m}}, \\ \delta_i+\dfrac{\bar{\delta}_{\mathrm{m}}}{k_\delta}, & |\lambda_{1i}|\leqslant\delta_{\mathrm{m}},\lambda_{2i}>\bar{\delta}_{\mathrm{m}}, \\ \delta_i+\dfrac{1}{k_\delta}[\dot{\delta}_{\mathrm{eq}i}+k_i\mathrm{sgn}(\sigma_i)], & |\lambda_{1i}|\leqslant\delta_{\mathrm{m}},|\lambda_{2i}|\leqslant\bar{\delta}_{\mathrm{m}}, \\ \delta_i-\dfrac{\bar{\delta}_{\mathrm{m}}}{k_\delta}, & |\lambda_{1i}|\leqslant\delta_{\mathrm{m}},\lambda_{2i}<-\bar{\delta}_{\mathrm{m}}, \\ -\delta_{\mathrm{m}}, & \lambda_{1i}<-\delta_{\mathrm{m}}. \end{cases} \tag{36}$$

where $\lambda_{1i}=\delta_i+\dfrac{\dot{\delta}_{\mathrm{eq}i}+k_i\mathrm{sgn}(\sigma_i)}{k_\delta}$, $i=1,2$,

$\lambda_{2i}=\dot{\delta}_{\mathrm{eq}i}+k_i\mathrm{sgn}(\sigma_i)$, $i=1,2$.

3 Adjustment Algorithm of Dynamic Boundary Layer

The continuous sliding mode control law of the rudder angle can avoid the chattering of sliding mode, but can not solve the problem caused by the amplitude and rate constraints of rudder actuator. Once the control input exceeds the amplitude and rate constraints of the rudder actuator, the sliding mode will fail and cause the system's tracking performance deterioration. The problem that the constraints of the rudder actuator are easily exceeded can be avoided effectively and the chattering phenomenon can also be eliminated through increasing the boundary layer thickness[18–19]. However, this method will reduce the system's tracking performance. Therefore, the dynamic adjustment method of the boundary layer thickness is used to solve the amplitude and rate constraints of the rudder actuator. Through a comprehensive analysis, the sliding boundary layer thickness ε_i requires to meet the following three conditions:

(1) In order to make the saturation function work in linear region so as to avoid the sliding mode controller saturated, the required condition can be expressed as

$$|\sigma_i|\leqslant\varepsilon_i,\ i=1,2. \tag{37}$$

Hence, $\varepsilon_i'=|\sigma_i|+l_i', l_i'\geqslant 0,\ i=1,2,3$.

(2) In order to meet the amplitude constraint of the rudder actuator, the required condition can be expressed as

$$\left|\delta_i+\frac{1}{k_\delta}\left[\dot{\delta}_{\mathrm{eq}i}+k_i\mathrm{sat}\left(\frac{\sigma_i}{\varepsilon_i}\right)\right]\right|\leqslant\delta_{\mathrm{m}},\ i=1,2. \tag{38}$$

Hence $\varepsilon_i''=\dfrac{k_i|\sigma_i|}{k_\delta\delta_{\mathrm{m}}-(k_\delta\delta_i+\dot{\delta}_{\mathrm{eq}i})\mathrm{sgn}(\sigma_i)}+l_i'',\ l_i''\geqslant 0, i=1,2.$

(3) In order to meet the rate constraint of the rudder actuator, the required condition can be expressed as

$$\left|\dot{\delta}_{\mathrm{eq}i}+k_i\mathrm{sat}\left(\frac{\sigma_i}{\varepsilon_i}\right)\right|\leqslant\bar{\delta}_{\mathrm{m}},\ i=1,2. \tag{39}$$

Hence $\varepsilon_i'''=\dfrac{k_i|\sigma_i|}{\bar{\delta}_{\mathrm{m}}-\dot{\delta}_{\mathrm{eq}i}\mathrm{sgn}(\sigma_i)}+l_i''',\ l_i'''\geqslant 0,\ i=1,2.$

The choice of dynamic boundary layer will be a trade-off between that avoiding the saturation of the sliding mode controller and reducing the domain of attraction, which can be expressed as

$$\varepsilon_i=\max\left\{\varepsilon_i',\varepsilon_i'',\varepsilon_i'''\right\},\ i=1,2. \tag{40}$$

It can be seen from Eq. (40), the on-line dynamic adjustment strategy of the boundary layer thickness can not only ensure the system's robustness about the parameters variation and disturbance, but also can avoid the system's performance degradation caused by the amplitude and rate constraints of the rudder actuator. Furthermore, this method does not require the work such as on-line parameters identification.

4 Verification and Analysis of Sliding Mode Controller Design Method

The sliding mode controller design method based on the dynamic boundary layer can be verified through comparison and analysis of the performance of the sliding mode controller at various situations. The state equation of the new AUV's yaw angle can be expressed as

$$\begin{pmatrix} \dot{\psi} \\ \dot{r} \end{pmatrix} = \boldsymbol{A}\begin{pmatrix} \psi \\ r \end{pmatrix} + \boldsymbol{B}\delta_r, \tag{41}$$

where ψ is the yaw angle of the new AUV, r is the yaw angular velocity of the new AUV, δ_r is the deflection angle of the vertical rudder actuator, $\boldsymbol{A}$ and $\boldsymbol{B}$ are known coefficient matrixes according to the design aim of the new AUV at the speed 10 m/s, $\boldsymbol{A} = \hat{\boldsymbol{A}} - \Delta\boldsymbol{A}$, $\boldsymbol{B} = \hat{\boldsymbol{B}} - \Delta\boldsymbol{B}$, $\hat{\boldsymbol{A}}$ and $\hat{\boldsymbol{B}}$ are the coefficient matrixes of the initial state, which can be written as

$$\hat{\boldsymbol{A}} = \begin{pmatrix} 1.07 & 0.04 \\ -1.82 & 0.07 \end{pmatrix},\ \hat{\boldsymbol{B}} = \begin{pmatrix} -0.78 \\ 0.90 \end{pmatrix}. \tag{42}$$

$\Delta\boldsymbol{A}$ and $\Delta\boldsymbol{B}$ describe the coefficient matrixes changes of the system at t=35 s, which can be written as

$$\Delta\boldsymbol{A} = \begin{pmatrix} 0.35 & 0.01 \\ -0.31 & 0.02 \end{pmatrix} \cdot (t-35),$$
$$\Delta\boldsymbol{B} = \begin{pmatrix} -0.39 \\ 0.45 \end{pmatrix} \cdot (t-35). \tag{43}$$

The efficiency of the rudder actuator is reduced by half to verify the robustness of the sliding mode controller about the unmodeled features and the external disturbance.

The maximum deflection angle and angular velocity of the vertical rudder actuator are designed as $\delta_{r\max} = 0.4$ and $\overline{\delta}_{r\max} = 0.9$, respectively. The kinematic equation of the vertical rudder can be expressed as

$$\dot{\delta}_r = -8\delta_r + 8u_c. \tag{44}$$

According to the sliding mode controller design method based on dynamic boundary layer, the angular velocity control command is computed with the yaw angle deviation firstly, and then the control input command of the vertical rudder actuator is computed with inner-loop sliding mode controller for angular velocity. In order to study the restraint effects of the controller on the amplitude and rate constraints of the rudder actuator and the impacts from the dynamic characteristics of the rudder actuator on the controller, assuming that the inner-ring angular velocity control command has been got by the outer-loop sliding mode controller, as shown in Fig. 3. Since the discontinuous angular velocity control command can not be used as the reference trajectory directly, a continuous command r_r filtered by the reference model is used as the reference trajectory[20]. The coefficient matrixes of the reference model are written as

$$\boldsymbol{A}_r = \begin{pmatrix} -0.53 & 0.24 \\ -0.97 & -0.69 \end{pmatrix},\ \boldsymbol{B}_r = \begin{pmatrix} 0 \\ 1.05 \end{pmatrix}. \tag{45}$$

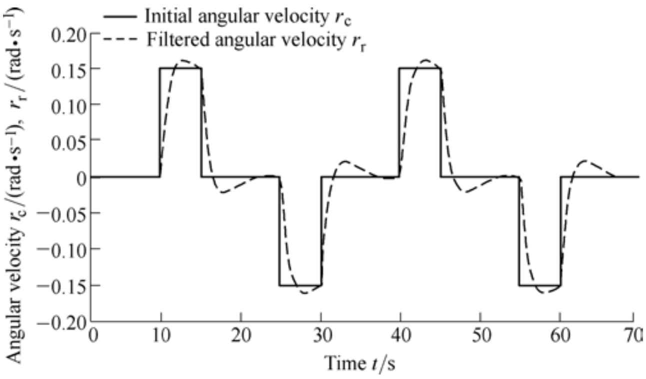

Fig. 3. Angular velocity reference control command

According to the design method of the inner-ring sliding mode controller, the sliding surface and sliding mode control law are designed respectively as

$$\sigma = 8(\dot{r}_r - \dot{r}) + 2(r_r - r) + 1.8\int (r_r - r)\mathrm{d}t, \tag{46}$$

$$u_c = \delta_r + 0.8\left[1.5 \cdot \mathrm{sat}\left(\frac{\sigma}{0.1}\right)\right]. \tag{47}$$

In order to demonstrate the effectiveness of the sliding mode controller based on dynamic boundary layer and analyze the impacts of system parameters, rudder actuator constraints and boundary layer on sliding mode controller, five instances are computed and analyzed respectively.

4.1 Considering dynamic characteristics of the vertical rudder

The state parameters of the system keep unchanged and the dynamic characteristics of the vertical rudder are considered, but not the vertical rudder's constraints. Static boundary layer is used.

The state parameters of the system are assumed to be unchanged. The dynamic characteristics of the vertical rudder are considered, but not the size of the amplitude and rate. Then the performance of the sliding mode controller is computed with static boundary layer. The computational results are shown in Fig. 4. It can be seen that the performance of the sliding mode controller is stable, which ensures the angular velocity output tracking the angular velocity reference command with high accuracy.

4.2 Changing parameters of the system

The state parameters of the system begin to change at t=35 s. The dynamic characteristics of the vertical rudder are considered, but not the vertical rudder's constraints. Static boundary layer is used.

The state parameters of the system begin to change at the t=35 s, namely reducing the efficiency of the vertical rudder by half. The robustness of the sliding mode controller about the fluctuations of the system state parameters is verified through considering the dynamic characteristics of the vertical rudder, while the size of the amplitude and rate is not considered. The static boundary layer is used in the computation. The computational results are shown in Fig. 5. It can be seen that the performance parameters of sliding mode controller have been changed after the system state parameters changing at t=35 s. The efficiency of the vertical rudder reduces significantly, as shown in Fig. 5(c) and Fig. 5(e), but the tracking error of the angular velocity reference command is only a small increase in magnitude of 10^{-4}, which shows that the robustness of the sliding mode controller about the perturbation of the system state parameters is good.

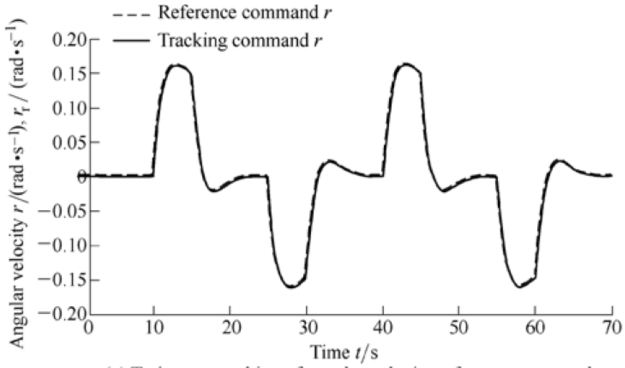

(a) Trajectory tracking of angular velocity reference command

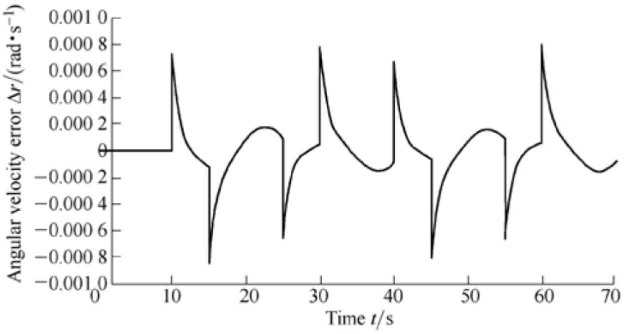

(b) Tracking error of angular velocity reference command

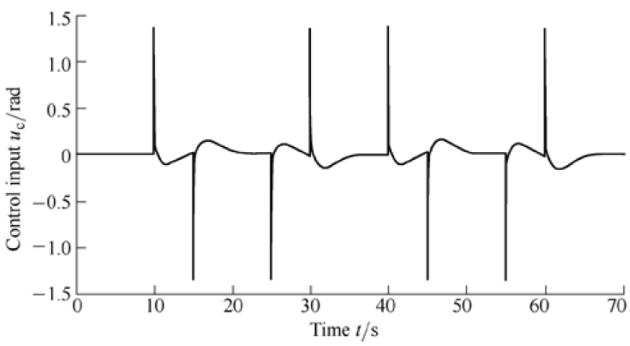

(c) Control input command of vertical rudder

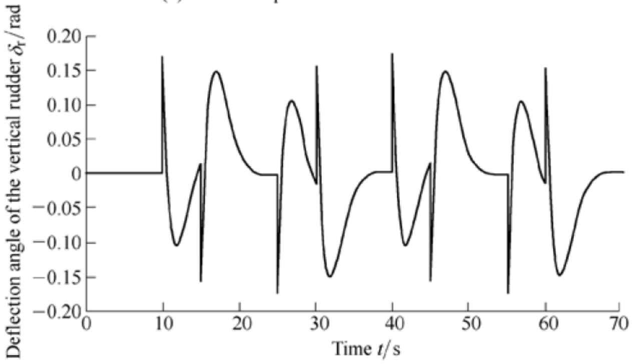

(d) Deflection angle of vertical rudder

Fig. 4. Performance of the sliding mode controller considering the vertical rudder's dynamic characteristics

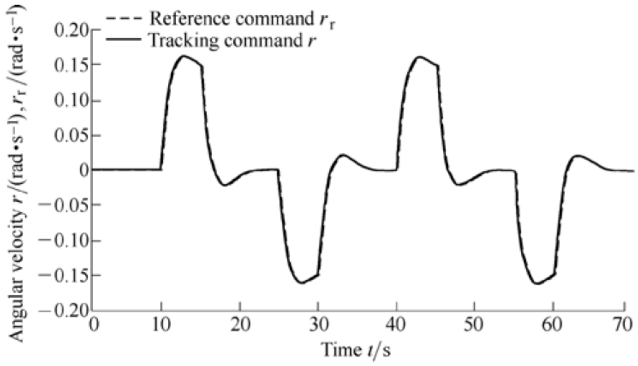

(a) Trajectory tracking of angular velocity reference command

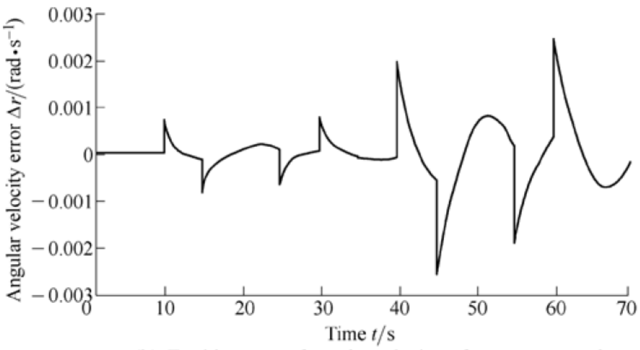

(b) Tracking error of angular velocity reference command

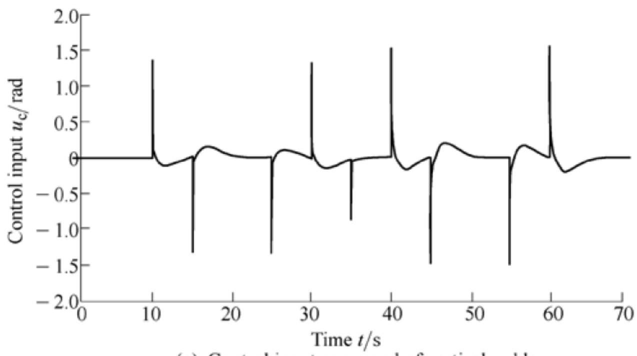

(c) Control input command of vertical rudder

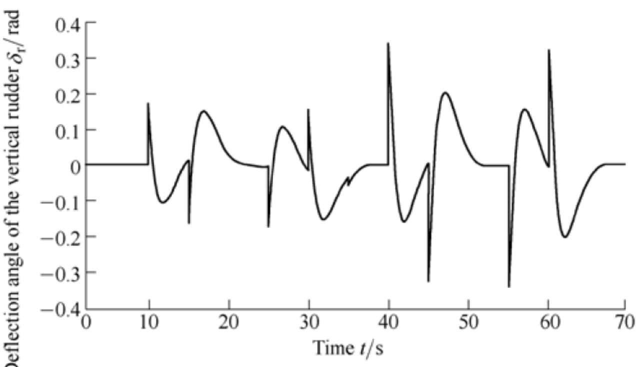

(d) Deflection angle of vertical rudder

Fig. 5. Performance of the sliding mode controller considering the state parameters change

4.3 Considering constraints of the vertical rudder

The state parameters of the system begin to change at t=35 s. The dynamic characteristics and constraints of the vertical rudder are considered. Static boundary layer is used.

In order to investigate the impacts of the amplitude and rate constraints of the vertical rudder on the sliding mode controller, the constraint conditions in Eq. (4) are met in the computation. Furthermore, the dynamic characteristics of the vertical rudder are considered and state parameters of the system change at t=35 s. The static boundary layer is also used in the computation. The computational results are shown in Fig. 6.

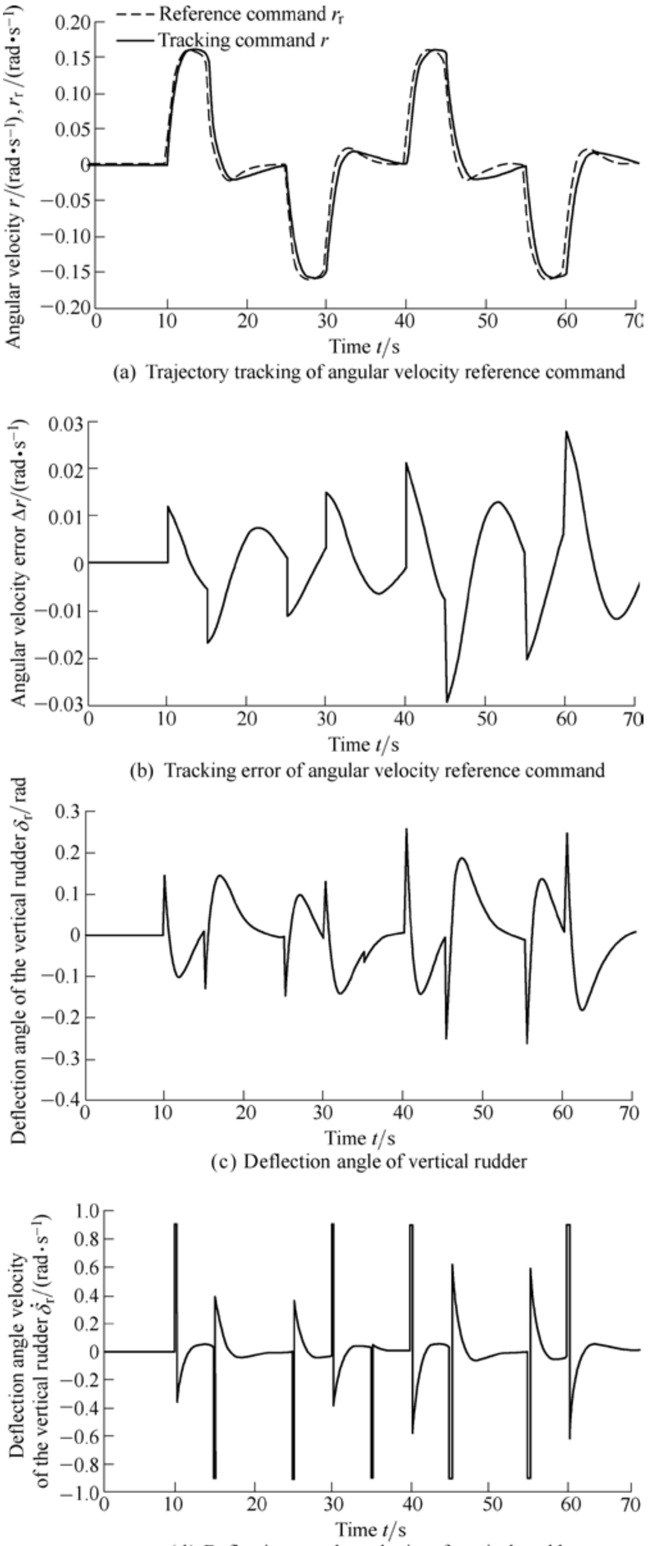

(a) Trajectory tracking of angular velocity reference command

(b) Tracking error of angular velocity reference command

(c) Deflection angle of vertical rudder

(d) Deflection angular velocity of vertical rudder

Fig. 6. Performance of the sliding mode controller exceeding the vertical rudder's rate constraint

It can be seen from Fig. 6 that the deflection rate of the vertical rudder exceeding constraint leads to the tracking performance of angular velocity reference command reducing significantly. The tracking error increases gradually after the system state parameters changing. Since the amplitude constraint of the vertical rudder has not been reached, the sliding mode controller can still track the angular velocity reference command stably, which shows that the rate constraint of the vertical rudder will lead to the performance of the sliding mode controller reducing, but will not compromise the stability of the system.

4.4 Outer-loop sliding mode control algorithm design for attitude angle

The amplitude of the angular velocity reference command is increased to $r_{\max}$=0.33 rad/s, the state parameters of the system begin to change at t=35 s. The dynamic characteristics and constraints of the vertical rudder are considered. Static boundary layer is used.

In order to examine the performance of sliding mode controller when the amplitude constraint of the vertical rudder is exceeded, the amplitude of the angular velocity reference command is increased to 0.33 rad/s, because the amplitude constraint of the vertical rudder will be easily exceeded through increasing the amplitude of the angular velocity reference command. Then the continuous reference command is got through filtering the reference command with the reference model. The other computational parameters are the same as the third case. The computational results are shown in Fig. 7. It can be seen that the divergence begins to appear when the amplitude constraint of the vertical rudder is exceeded and the system can not continue to track the reference command, which shows the amplitude constraint of the vertical rudder has great impact on the stability of the sliding mode controller using static boundary layer.

4.5 Outer-loop sliding mode control algorithm design for attitude angle

The amplitude of the angular velocity reference command is increased to $r_{\max}$=0.33 rad/s, the state parameters of the system begin to change at t=35 s. The dynamic characteristics and constraints of the vertical rudder are considered. Dynamic boundary layer is used.

In order to solve the problem caused by the amplitude and rate constraints of the rudder actuator, according to the definition in Eq. (37), Eq. (38) and Eq. (39), three boundary layers meeting the conditions are selected and the maximum value method is used to achieve dynamic boundary layer, the other computational parameters are the same as the fourth case.

$$\varepsilon' = |\sigma| + 0.02, \tag{48}$$

$$\varepsilon'' = \frac{1.5|\sigma|}{1.25\cdot 0.4 - 1.25\delta_r \mathrm{sgn}(\sigma)} + 0.02, \tag{49}$$

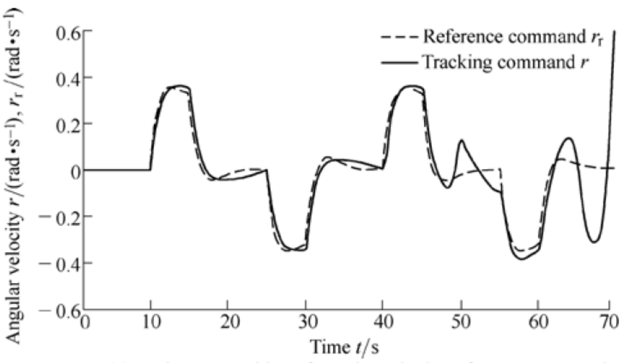

(a) Trajectory tracking of angular velocity reference command

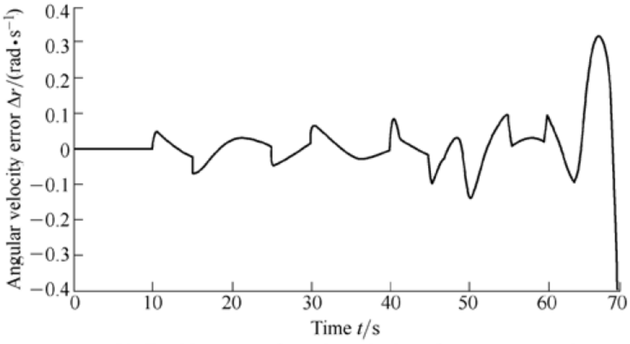

(b) Tracking error of angular velocity reference command

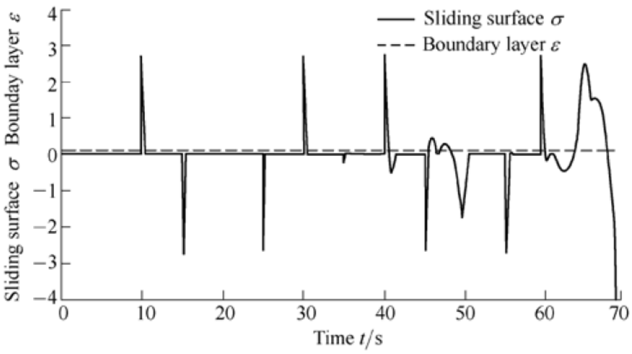

(c) Sliding surface and boundary layer of sliding mode controller

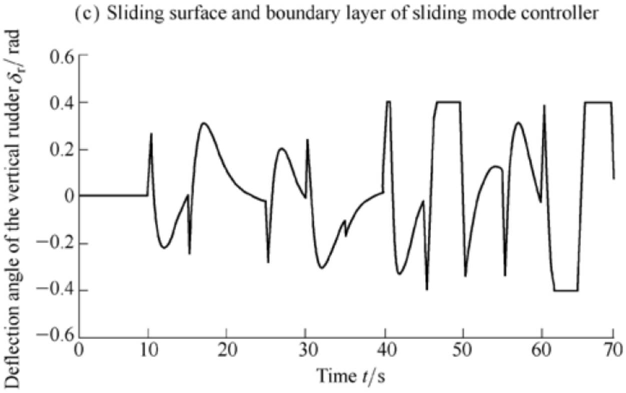

(d) Deflection angle of vertical rudder

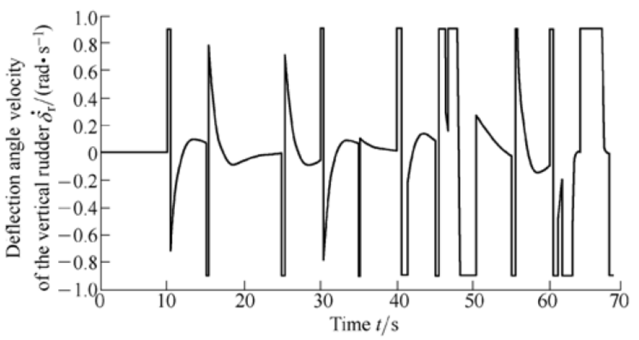

(e) Deflection angular velocity of vertical rudder

Fig. 7. Performance of the sliding mode controller exceeding the vertical rudder's amplitude constraint

$$\varepsilon''' = \frac{1.5|\sigma|}{0.9} + 0.02 , \tag{50}$$

$$\varepsilon = \max\left\{\varepsilon', \varepsilon'', \varepsilon'''\right\} , \tag{51}$$

The computational results are shown in Fig. 8. It can be seen that foregoing divergent system using static boundary layer resumes stabilization when the dynamic boundary layer is used and the satisfactory tracking performance is obtained under the amplitude and rate constraints of the vertical rudder. Compared with the fourth case, the tracking error of the system and the amplitude of the vertical rudder are reduced. Furthermore, the deflection angle of the vertical rudder has not yet reached its amplitude constraint. The angular rate of the vertical rudder is greatly improved, though it still exceeds the rate constraint. The results show that the dynamic boundary layer has very important significance on maintaining the stability of the sliding mode controller under the amplitude and rate constraints of rudder actuator.

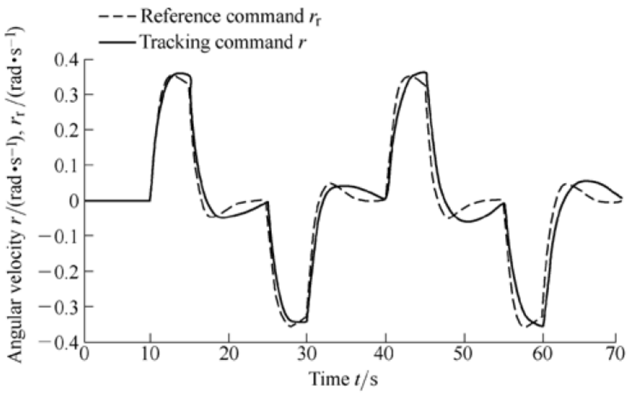

(a) Trajectory tracking of angular velocity reference command

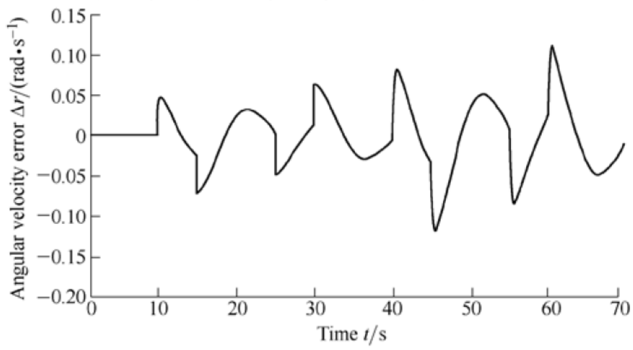

(b) Tracking error of angular velocity reference command

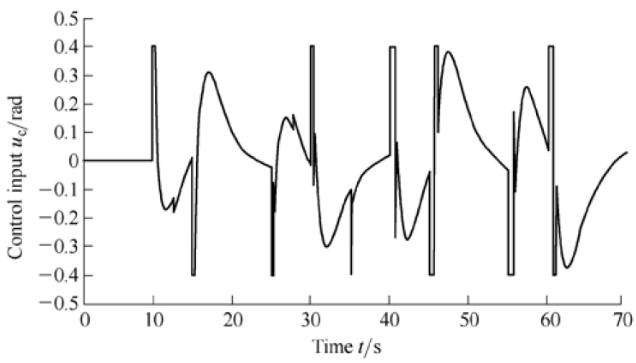

(c) Control input command of vertical rudder

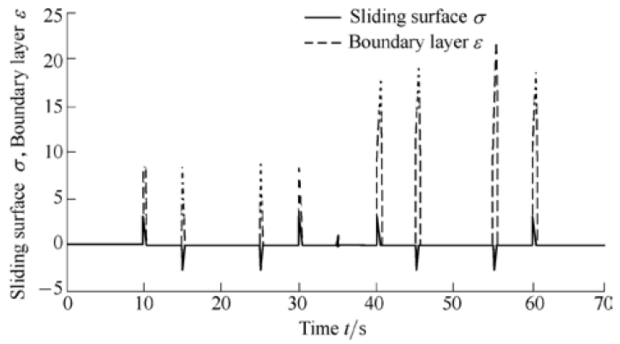

(d) Sliding surface and boundary layer of sliding mode controller

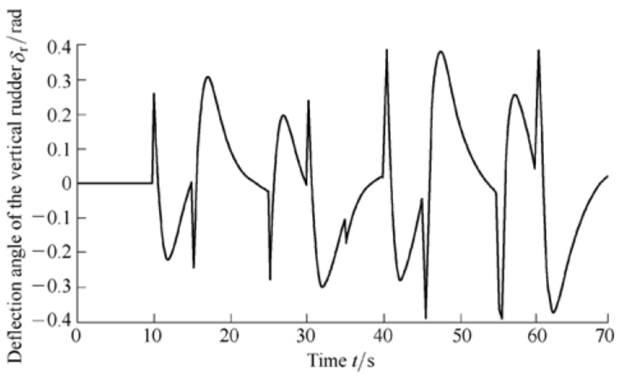

(e) Deflection angle of vertical rudder

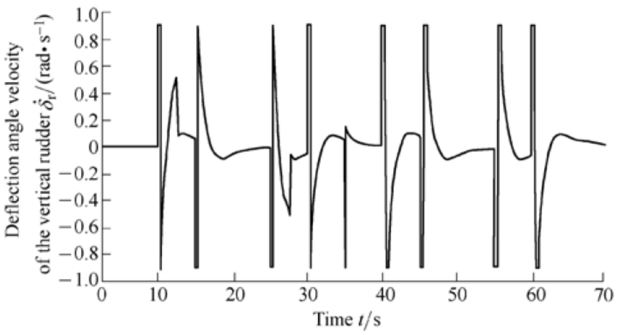

(f) Deflection angular velocity of vertical rudder

Fig. 8. Performance of the sliding mode controller applying the dynamic boundary layer

5 Conclusions

(1) A second-order sliding mode controller with double-loop structure that considering the dynamic characteristics of the rudder actuator is designed, which manages to solve the nonlinear term, unmodeled dynamics and external disturbances caused by the marine environment. The stability of the system is analyzed based on Lyapunov stability theory so as to ensure the robustness of the system and avoid the control failure caused by the unconformity between the sliding mode controller design theory and the actual application conditions.

(2) In order to avoid the loss of the sliding mode caused by the amplitude and rate constraints of the rudder actuator in the attitude control of the new AUV, the dynamic boundary layer is used to dynamically adjust the thickness of the sliding boundary layer so as to obtain the best anti-chattering effects. Hence, the foregoing divergent second-order sliding mode controller can still effectively implement the attitude control of the AUV, which ensures the stability of the system and does not exceed the amplitude constraint of the rudder actuator.

(3) The impacts of system parameters, rudder actuator's constraints and boundary layer on the sliding mode controller are computed and analyzed to verify the effectiveness and robustness of the sliding mode controller based on dynamic boundary layer, which provides a theoretical guidance and technical support for the control system design of the new AUV in real complex sea conditions.

References

[1] PAN C Y, WEN X S. Research on transmission principle and kinematic analysis for involute spherical gear[J]. *Journal of Mechanical Engineering*, 2005, 41(5): 1–9. (in Chinese)

[2] GAO F D, PAN C Y, XU H J, et al. Design and mechanical performance analysis of a new wheel propeller[J]. *Chinese Journal of Mechanical Engineering*, 2011, 24(5): 805–812.

[3] YOUNG K D, UTKIN V I, OZGUNER U. A control engineer's guide to sliding mode control[J]. *IEEE Transactions on Control Systems Technology*, 1999, 7(3): 328–342.

[4] PERRUQUETTI W, BARBOT J P. *Sliding mode control in engineering*[M]. New York: Marcel Dekker Inc., 2002.

[5] SHTESSEL Y B, BUFFINGTON J M, BANDA S S. Multiple time scale flight control using reconfigurable sliding modes[J]. *Journal of Guidance, Control and Dynamics*, 1999, 22(6): 873–880.

[6] MACRO D B, HEALEY A J. Command control and experiment results with the NPS ARIES AUVs[J]. *IEEE Journal of Oceanic Engineering*, 2001, 26(4): 466–475.

[7] LIU B, YAN W S, CUI R X. Second-order sliding mode control of autonomous underwater vehicles[J]. *Journal of Projectiles, Rockets, Missiles and Guidance*, 2005, 25(4): 321–323. (in Chinese)

[8] GAO J, XU D M, LI J, et al. Adaptive backstepping sliding mode control for surge motion of an autonomous underwater vehicle[J]. *Journal of Northwestern Polytechnical University*, 2007, 25(4): 552–555. (in Chinese)

[9] YAN W S, GAO J, YANG L, et al. Longitudinal sliding mode control of a new type long distance autonomous underwater vehicle[J]. *Journal of Northwestern Polytechnical University*, 2007, 25(4): 538–542. (in Chinese)

[10] CHEN M S, HWANG Y R, TOMIZUKA M. A state-dependent boundary layer design for sliding mode control[J]. *IEEE Transactions on Automatic Control*, 2002, 47(10): 1 677–1 681.

[11] VICENTE P V, GERD H. Chattering-free sliding mode control for a class of nonlinear mechanical systems[J]. *International Journal of Robust and Nonlinear Control*, 2001, 11(12): 1 161–1 178.

[12] SESHAGIRI S, KHALIL H K. On introducing integral action in sliding mode control [C]//*Proceedings of the 41st IEEE Conference on Decision and Control*. 2002, Dec. 10–13, East Lansing, MI, USA, 2002: 1 473–1 478.

[13] GAO F D PAN C Y, YANG Z, et al. Nonlinear mathematics modeling and analysis of the vectored thruster autonomous underwater vehicle in 6-DOF motions[J]. *Journal of Mechanical Engineering*, 2011, 47(5): 93–100. (in Chinese)

[14] MASON P, SIGALOTTI M, DAAFOUZ J. On stability analysis of linear discrete time switched system using quadratic Lyapunov functions[C]//*Proceedings of the 46st IEEE Conference on Decision and Control*, 2007, Dec. 12–14, New Orleans, LA, USA, 2007: 5 629–5 633.

[15] XU R, OZGUNER U. Sliding mode control of a class of underactuated systems[J]. *Automatic*, 2008, 44(1): 233–241.

[16] BESSA W M, DUTRA M S, KREUZER E. An adaptive fuzzy sliding mode controller for remotely operated underwater vehicles[J]. *Robotics and Autonomous Systems*, 2010, 58(1): 16–26.
[17] HEALY A J, LIENARD D. Multivariable sliding mode control for autonomous diving and steering of unmanned underwater vehicles[J]. *IEEE Journal of Oceanic Engineering*, 1993, 18(3): 327–339.
[18] MACRO D B, HEALEY A J. Command control and experiment results with the NPS ARIES AUVs[J]. *IEEE Journal of Oceanic Engineering*, 2001, 26(4): 466–475.
[19] VICENTE P V, GERD H. Chattering-free sliding mode control for a class of nonlinear mechanical systems[J]. *International Journal of Robust and Nonlinear Control*, 2001, 11(12): 1 161–1 178.
[20] LAPIERRE L, JOUVENCEL B. Robust nonlinear path-following control of an AUV[J]. *IEEE Journal of Oceanic Engineering*, 2008, 33(2): 89–102.

Biographical notes

GAO Fudong, born in 1982, is currently a PhD candidate at *College of Mechatronic Engineering and Automation*, *National University of Defense Technology*, *China*. He received his bachelor degree and master degree in 2005 and 2007, respectively from *National University of Defense Technology, China*. His research interests include computational fluid dynamics, design and performance prediction of submerged weapons.
Tel: +86-731-84574932; E-mail: gaofudong2005@163.com

PAN Cunyun, born in 1955, is currently a professor at *National University of Defense Technology*, *China*. His research interests include mechachonics engineering, ocean engineering and mechanical design theory.
Tel: +86-731-84576481; E-mail: pancunyun@sina.com

HAN Yanyan, born in 1985, is currently an engineer at *SANY Heavy Industry Co. Ltd, China.* Her research interests include mechachonics engineering and mechanical design theory.
Tel: +86-731-84031778; E-mail: hanyanyan541@163.com